Solutions of Nonlinear Free Vibration of Single-Walled Carbon Nanotubes Conveying Fluid

G. Venkatraman* and D. Suji

PSG College of Technology, Avinasi road, Coimbatore-641016, Tamilnadu, India

Received: 06.12.2021 & Accepted: 14.01.2022

Doi: 10.12693/APhysPolA.141.218 *e-mail: gvr.civil@psgtech.ac.in

Flow-induced vibration of carbon nanotubes becomes an important topic in nanotechnology. In our study, the non-linear vibrational behaviour of single-walled carbon nanotubes is presented. A single-walled carbon nanotube is modelled as a simply supported beam embedded in the Winkler–Pasternak foundation. For the analysis, the Euler–Bernoulli beam theory is used to develop the model. This study uses a continuum approach which is widely employed for the dynamic behaviour of carbon nanotubes. The governing non-linear equation of motion is solved using the homotopy perturbation method. Elliptical functions are used to solve the exact solutions of these differential equations. The results of the exact solutions in terms of elliptic functions are compared to both the linear and non-linear frequencies. Concerning changes in the Winkler and Pasternak parameters, axial force and flow velocity, the variation between linear and non-linear frequencies is studied. Furthermore, by adjusting these parameters, the non-linear vibrational frequency can be fine-tuned.

topics: vibration of SWCNT, nonlinear free vibration, exact solution, elliptical function method

1. Introduction

Fluid conveyance devices made of carbon nanotubes (CNTs) are frequently employed in nanotechnology. The remarkable mechanical, electrical, chemical and physical capabilities of CNTs have made them suitable for a wide range of novel nanotechnology applications. CNTs are also employed as nanopipes and nanotubes due to their hollow cylindrical shape and extraordinarily high elasticity and flexibility.

Flow-induced vibration of CNTs becomes an important topic in nanotechnology. Molecular dynamics (MD) simulation and continuum approach are the two most common approaches used to examine vibrational behaviour of nanotubes. Continuum theories are frequently and effectively utilised to model the dynamical behaviour of CNTs since MD simulation is still time-consuming and requires a lot of computational work, even for smaller nanostructures. The flow-induced vibration will be affected by the viscosity of the fluid, the aspect ratio of CNT, and the elastic medium constants. Because CNTs are frequently embedded in a foundation, the mechanical characteristics of the medium have a substantial impact on the dynamic behaviour of nanotubes. The Winkler-type foundation, which replicates an elastic medium as a collection of closely spaced, mutually independent vertical springs, is frequently used to describe the interaction between the foundation and the CNT. However, because this model shapes the foundation as a discontinuous and incoherent medium, it is unable to accurately determine the mechanical behaviour. The Pasternak-type foundation model represents a more exact and generalised medium simulation by using two independent parameters (called the Pasternak parameters). Normal pressure is the first parameter, followed by shear resistance, which is determined by the elastic medium's interaction with the shear deformation.

The vibration of CNTs was studied using several theories and different types of supporting media, both in linear and non-linear formulations. Traditional perturbation methods are used to solve the final equation of motion. The most significant drawback of perturbation approaches is that the solution is entirely dependent on the small perturbation parameter and is therefore only applicable to weak non-linear situations. Approximate variational approaches, which are unique and simple techniques with reasonably accurate findings, can be employed instead of the classic perturbation methods to obtain the analytical solution for highly non-linear models. Approximate variational methods such as variational iteration, homotopy perturbation, parameter expansion, max-min method, and energy balance approach have been widely and successfully used in a variety of non-linear mathematical, physical, and engineering applications.

In this work, non-linear vibration of single-walled carbon nanotube (SWCNT) conveying fluid over a Pasternak-type elastic basis is simulated using continuum theory. The flow-induced vibrational

behaviour of single-walled carbon nanotubes is investigated using the Euler–Bernoulli elastic theory. The homotopy perturbation method is used to solve the non-linear equation of motion. The Jacobian elliptical functions are used to solve exact solutions of these dynamic equations. The results of exact solutions in terms of elliptic functions are compared with the solved linear and vibrational frequencies. Concerning changes in the Winkler and Pasternak parameters, axial force, and flow velocity, the variation between linear and non-linear frequencies is investigated. Furthermore, by adjusting these parameters, the non-linearity of the model can be fine-tuned.

Several analytical investigations of the vibrational behaviour of carbon nanotubes have been conducted in the last few decades, and their solutions to non-linear equations are studied and compared with other techniques. Homotopy perturbation technique was introduced in 1990s by J.M. He [1], who explained the basic concept of the homotopy perturbation approach and demonstrated it for certain cases. J.H. He [1] concluded that since the new method does not require small parameters in the equations, it can overcome the limitations of previous perturbation methods. The homotopy perturbation method yields approximations that are valid not just for small but also for very large values. In addition, their first-order approximations are highly precise.

J.H. He introduced the variational iteration approach — a novel type of analytical tool for non-linear problems — which provides an approximate solution for some well-known non-linear problems [2]. J.H. He concludes that a correction functional can be quickly generated by a general Lagrange multiplier, and the multiplier can be optimized by examining several situations using the variational iteration method. The introduction of constrained variations in the corrective functional makes it easier to determine the multiplier. When compared to Adomian's technique, the approximations obtained by this method converge to the exact answer faster than Adomian's.

In [3], J.H. He applied the homotopy perturbation approach to a Duffing equation with a high order of non-linearity to show how effective and convenient this approach is. The results show that the proposed method's first-order approximation is valid even for very large non-linear parameters and is more accurate than the perturbation solutions at the second order of approximation. In [4], J.H. He used the homotopy perturbation method to solve non-linear boundary value problems and compared the results with the various methods and revealed that the present method is very effective and convenient.

Erignen's nonlocal elasticity theory is used to create a non-linear model for the vibration of a single-walled carbon nanotube by Soltani and Farshidianfar [5]. With simple boundary constraints, the nanotube is immersed in a Pasternak-type foundation. The non-linear equation of motion is solved using the energy balance method (EBM) to get a precise flow-induced frequency. The results reveal that by introducing axial stress to the nanotube, the model's non-linearity may be efficiently controlled.

Later, Natsuki et al. [6] demonstrated a wave propagation methodology for the vibrational analysis of fluid-filled double-walled carbon nanotubes. The governing equations of vibration for carbon nanotubes were simplified by the shell equations. The van der Waals interaction between two nearby carbon nanotubes is used to model the double-walled carbon nanotubes as a two-shell model.

The effect of the internal flowing fluid and compressive axial load on the non-linear vibration and stability of embedded carbon nanotubes was studied by Rasekh and Khadem [7]. The vibrational behaviour of the embedded carbon nanotube is modelled using the Euler–Bernoulli beam theory. A multiple scales perturbation approach is used to analyse the problem. The surrounding elastic media is found to play a significant role in the carbon nanotube's stability.

The influence of an internal moving fluid on free vibration and flow-induced structural instability of carbon nanotubes is investigated by Yoon et al. [8]. The influence of the resonant frequencies on the flow velocity is illustrated in detail, and the critical flow velocity at which the structural instability of carbon nanotubes develops is estimated. To examine the dynamic behaviour of an inclined SWCNT subjected to a viscous fluid flow, Kiani [9] proposed a mathematical model and studied all parameters affecting the frequency of vibration. The size-dependent non-linear free vibration and instability of fluid-conveying single-walled boron nitride nanotubes (SWBNNTs) in a thermal environment is investigated by Ansari et al. [10]. The problem is solved by the generalized differential quadrature method. The effects of different parameters on instability and vibration are studied in detail.

Hosseini and Sadeghi-Goughari [11] analysed the instability and vibration characteristics of fluid conveying carbon nanotube under a longitudinal magnetic field. They concluded that a strong magnetic field decreases the interior fluid flow. Using a nonlocal continuum theory, Wang et al. [12] studied the effect of non-linear vibration of carbon nanotube embedded in a viscous elastic matrix. Based on the findings, it can be concluded that parametric excitation can drastically alter the stable zone.

Geometric non-linear nonlocal model of supported carbon nanotubes transporting fluid is derived and analytical solutions were found by Dai et al. [13]. The nonlocal effect is shown to have a considerable impact on the nanotube's natural frequencies before and after buckling. Recently, many researchers [14–16] studied the linear and non-linear vibration characteristics of functionally graded nanoshells conveying fluid.

2. Mathematical modelling

Figure 1 shows a hollow cylindrical tube of single-walled carbon nanotubes carrying fluid in a Pasternak-type elastic media. The Euler–Bernoulli beam theory is employed to simulate the vibrational behaviour of the nanotube, which is based on the assumption that it is simply supported at both ends.

The small scale effects are significant in the vibration of SWCNT conveying fluid, Eringen nonlocal continuum theory is used, based on the nonlocal continuum theory of Eringen titled "Stress at a point depends on strain field at every point in the body". The relationship between a nonlocal stress tensor (σ') and a local stress tensor (σ) is expressed as

$$\left(1-(e_0\,a)^2\,\nabla^2\right)\sigma=\sigma', \tag{1}$$

where (e_0a) is the small scale parameter, e_0 is a constant, and ∇^2 is the Laplacian operator.

Using Newton's law, the governing equation of the transverse motion of an SWCNT conveying fluid can be expressed as [5]

$$\frac{\partial Q}{\partial x}=m_c\frac{\partial^2 w}{\partial t^2}+k_e\,w-k_p\frac{\partial^2 w}{\partial x^2}+F\frac{\partial^2 w}{\partial x^2}+F_w, \tag{2}$$

where x is the axial coordinate, t denotes time, $w(x,t)$ denotes the SWCNT transverse deflection, m_c is the mass of the nanotube per unit length, k_e and k_p are the Pasternak parameters representing the Winkler and Pasternak constants, F is the transverse shear force whereas Q represents the applied axial tension. Force per unit length induced by the fluid flow is represented by F_w here and is given as

$$F_w=m_f\left(2\mu\frac{\partial^2 w}{\partial x\partial t}+\mu^2\frac{\partial^2 w}{\partial x^2}+\frac{\partial^2 w}{\partial t^2}\right), \tag{3}$$

where m_f is the mass of the fluid per unit length of an SWCNT, and μ is the uniform mean flow velocity.

The transverse shear force Q, the bending moment M of the model, and the longitudinal force N are related by the Euler–Bernoulli beam theory as follows

$$\frac{\partial Q}{\partial x}=\frac{\partial^2 M}{\partial x^2}+N\frac{\partial^2 w}{\partial x^2}, \tag{4}$$

where

$$M=\int \mathrm{d}A_c\,z\,\sigma_{xx}=\int \mathrm{d}A_c\,zE\,\varepsilon_{xx}, \tag{5}$$

$$N=\int \mathrm{d}A_c\,\sigma_{xx}=\int \mathrm{d}A_c\,E\,\varepsilon_{xx}. \tag{6}$$

Using nonlocal realtionships from (1), the moment relationship can be written as

$$\left(1-(e_0a)^2\nabla^2\right)M=\int \mathrm{d}A_c\,zE\,\varepsilon_{xx}. \tag{7}$$

The axial strain and axial stress on the nanotube are represented by ε_{xx} and σ_{xx}, respectively. The distance from the neutral axis is represented by z, while the cross-section of the nanotube is represented by A_c.

The displacement field is given by

$$\begin{aligned} u(x,y,z,t)&=u(x,t)-z\frac{\partial w(x,t)}{\partial x},\\ w(x,y,z,t)&=w(x,t). \end{aligned} \tag{8}$$

The longitudinal displacement is denoted by u. The strain displacement relation is given by

$$\varepsilon_{xx}=\varepsilon_{x0}+z\,\kappa_x=\frac{\partial u}{\partial x}+\frac{1}{2}\left(\frac{\partial w}{\partial x}\right)^2-z\frac{\partial^2 w}{\partial x^2}. \tag{9}$$

Substituting (9) into (7), we get

$$\left(1-(e_0a)^2\nabla^2\right)M=E\,I\,\frac{\partial^2 w}{\partial x^2}. \tag{10}$$

Here, I is the second moment of the area with respect to center. The longitudinal displacement u can be expressed as a function of the transverse displacement w and axial tension F [5] as follows

$$u=\frac{xF}{EA_c}-\frac{1}{2}\int_0^x \mathrm{d}x\left(\frac{\partial w}{\partial x}\right)^2+\frac{x}{2L}\int_0^L \mathrm{d}x\left(\frac{\partial w}{\partial x}\right)^2. \tag{11}$$

The longitudinal force N is expressed as follows [5]

$$N=F+\frac{EA_c}{2L}\int_0^L \mathrm{d}x\left(\frac{\partial w}{\partial x}\right)^2. \tag{12}$$

Substituting (12) and (2) into (4) and using (3), the non-linear governing equation of motion is expressed as

$$\begin{aligned} &m_c\frac{\partial^2 w}{\partial x^2}+EI\frac{\partial^4 w}{\partial x^4}+k_e w-k_p\frac{\partial^2 w}{\partial x^2}+F\frac{\partial^2 w}{\partial x^2}+m_f\left(2\mu\frac{\partial^2 w}{\partial x\partial t}+\mu^2\frac{\partial^2 w}{\partial x^2}+\frac{\partial^2 w}{\partial t^2}\right)-\frac{EA_c}{2L}\frac{\partial^2 w}{\partial x^2}\int_0^L \mathrm{d}x\left(\frac{\partial w}{\partial x}\right)^2\\ &-(e_0a)^2\frac{\partial^2}{\partial x^2}\left[m_c\frac{\partial^2 w}{\partial x^2}+EI\frac{\partial^4 w}{\partial x^4}+k_e w-k_p\frac{\partial^2 w}{\partial x^2}+F\frac{\partial^2 w}{\partial x^2}+m_f\left(2\mu\frac{\partial^2 w}{\partial x\partial t}+\mu^2\frac{\partial^2 w}{\partial x^2}+\frac{\partial^2 w}{\partial t^2}\right)\right.\\ &\left.-\frac{EA_c}{2L}\frac{\partial^2 w}{\partial x^2}\int_0^L \mathrm{d}x\left(\frac{\partial w}{\partial x}\right)^2\right]=0. \end{aligned} \tag{13}$$

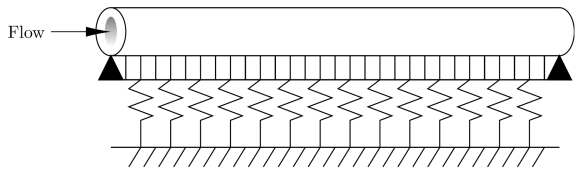

Fig. 1. A single walled carbon nanotube embedded in a Pasternak type foundation model characterized by the Winkler (k_e) and Pasternak (k_p) constant.

The boundary conditions of the simply supported SWCNT is written as

$$\begin{aligned} w(0,t) &= \frac{\partial^2 w(0,t)}{\partial x^2} = 0 \quad \text{at } x = 0, \\ w(L,t) &= \frac{\partial^2 w(L,t)}{\partial x^2} = 0 \quad \text{at } x = L. \end{aligned} \tag{14}$$

One can express $w(x,t)$ as the two independent functions of time and space, i.e.,

$$w(x,t) = q(t)\,\phi(x), \tag{15}$$

where ϕ is the normalized mode shape from the linear vibration analysis. Substituting (15) into (13), we have

$$\ddot{q}(t) + \frac{1+(1+e^2)(K_e+K_p-T-U^2)}{1+e^2}\,\omega_0^2\,q(t) + \frac{\omega_0^2}{4r^2}\,q^3(t) = 0. \tag{16}$$

The dimensionless parameters and variables are defined as follows

$$\begin{aligned} &\omega_0 = \frac{\pi^2}{L^2}\sqrt{\frac{EI}{m_c+m_f}}, \quad e = \frac{\pi}{L}\,e_0 A, \quad r = \sqrt{\frac{I}{A_c}}, \\ &K_e = \frac{L^4}{\pi^4}\frac{1}{EI}\,k_e, \quad K_p = \frac{L^2}{\pi^2}\frac{1}{EI}\,k_p, \\ &T = \frac{L^2}{\pi^2}\frac{1}{EI}\,F, \quad U = \frac{L}{\pi}\sqrt{\frac{m_f}{EI}}\,\mu. \end{aligned} \tag{17}$$

3. Solution

3.1. Homotopy perturbation technique

Traditional perturbation methods and homotopy techniques are fully utilized in the presented homotopy perturbation method. This method overcomes the drawbacks of the traditional perturbation methods and accurately predicts non-linear system behaviour. Let us consider the following non-linear differential equation, i.e.,

$$A(u) + f(r) = 0, \tag{18}$$

where A is a general differential operator, $f(r)$ is a known analytic function.

The operator A can be divided into two parts L and N, where L is linear and N is non-linear. Therefore, (18) can be rewritten as follows

$$L(u) + N(u) - f(r) = 0. \tag{19}$$

By the homotopy technique, we construct a homotopy of (18) which satisfies both,

$$H(v,p) = (1-p)\big[L(v) - L(u_0)\big] + p\,\big[A(v) - f(r)\big], \tag{20}$$

and

$$H(v,p) = L(v) - L(u_0) + p\,L(u_0) + p\,\big[N(v) - f(r)\big], \tag{21}$$

where $p \in (0,1)$ is an embedding parameter, and u_0 is an initial approximation that satisfies the boundary conditions.

From (20) and (21), one has

$$\begin{aligned} &\text{for } p = 0, \quad H(v,0) = L(v) - L(u_0) = 0, \\ &\text{for } p = 1, \quad H(v,1) = A(v) - f(r) = 0. \end{aligned} \tag{22}$$

The solution can be expressed as

$$v = v_0 + p\,v_1 + p^2 v_2 + \ldots \tag{23}$$

The approximate solution of (18), therefore, can be readily obtained as follows

$$u = v_0 + v_1 + v_2 + \ldots \tag{24}$$

The flow-induced non-linear frequency of CNT can be determined by solving the non-linear equation of motion.

The governing differential equation of motion is

$$\ddot{q}(t) + \frac{1+(1+e^2)(K_e+K_p-T-U^2)}{1+e^2}\,\omega_0^2 q(t) + \frac{\omega_0^2}{4r^2}q^3(t) = 0. \tag{25}$$

The initial conditions are

$$q(0) = a_0, \qquad \dot{q}(0) = 0. \tag{26}$$

The approximate solution is expressed as

$$q(t) = a_0\,\cos(\omega t), \tag{27}$$

where ω is the non-linear flow-induced frequency and a_0 is the initial amplitude of the vibration. Therefore, the homotopy of (25) can be written as

$$L(v) - L(q_0) + p\,L(q_0) + p\,\varepsilon\,v^3 = 0, \tag{28}$$

where $L(q) = \ddot{q}(t) + \frac{1+(1+e^2)(K_e+K_p-T-U^2)}{1+e^2}\omega_0^2 q(t)$ and $\varepsilon = \frac{\omega_0^2}{4r^2}$. By the homotopy manipulation as before, we have the following linear systems

$$\begin{aligned} &L(v_0) - L(q_0) = 0, \quad v_0(0) = a_0, \quad v_0'(0) = 0, \\ &L(v_1) + L(q_0) + \varepsilon\,v_0^3 = 0, \quad v_1'(0) = v_1(0) = 0. \end{aligned} \tag{29}$$

We set $v_0(t) = q_0(t) = a_0\cos(\omega t)$ as the initial approximation of (28). Therefore, from (29), we have

$$\frac{\partial^2 v_1}{\partial t^2} + \frac{1+(1+e^2)(K_e+K_p-T-U^2)}{1+e^2}\omega_0^2 v_1 + a_0\left(1-\omega^2+\frac{3\varepsilon a_0^2}{4}\right)\cos(\omega t) + \frac{\varepsilon a_0^3}{4}\cos(3\omega t) = 0. \tag{30}$$

The solution of (30) can be readily obtained from the variational iteration method [2] as follows

$$v_1(t) = \int^t \mathrm{d}t\, \sin(\tau - t)\left[\left(-\omega^2 + \frac{1+(1+e^2)(K_e+K_p-T-U^2)}{1+e^2}\omega_0^2 + \frac{3}{4}\varepsilon a_0^2\right)a_0\, \cos(\omega\tau)\frac{\varepsilon a_0^3}{4}\cos(3\omega t)\right] =$$
$$\left(-\omega^2 + \frac{1+(1+e^2)(K_e+K_p-T-U^2)}{1+e^2}\omega_0^2 + \frac{3}{4}\varepsilon a_0^2\right)\frac{a_0\left(\cos(\omega t)-\cos(t)\right)}{\omega^2-1}\,\frac{\varepsilon a_0^3\left(\cos(3\omega t)-\cos(t)\right)}{4(9\omega^2-1)}. \tag{31}$$

The constant ω can be identified by various methods such as the weighted residual method (least-squares method, method of collocation, the Galerkin method). For this, we will use a very simple technique to determine the constant. To eliminate the secular term which may occur in the next iteration, we set the coefficient which multiplies the cosines to zero. Thus,

$$\left(-\omega^2 + \frac{1+(1+e^2)(K_e+K_p-T-U^2)}{1+e^2}\omega_0^2 + \frac{3\varepsilon a_0^2}{4}\right)\frac{a_0}{\omega^2-1} + \frac{\varepsilon a_0^3}{4(9\omega^2-1)}. \tag{32}$$

From (32), the non-linear frequency ω can be expressed as

$$\omega = \sqrt{\frac{1+(1+e^2)(K_e+K_p-T-U^2)}{1+e^2}\omega_0^2 + \frac{3}{4}\varepsilon a_0^2}. \tag{33}$$

The linear frequency ω_L can be obtained by removing the non-linear terms and it has the following form

$$\omega = \sqrt{\frac{1+(1+e^2)(K_e+K_p-T-U^2)}{1+e^2}\,\omega_0^2}. \tag{34}$$

To show the pure non-linearity effect, "the non-linear frequency variation" $\Delta\omega$ [%] is defined

$$\Delta\omega = \frac{\omega-\omega_L}{\omega_L}\times 100. \tag{35}$$

This parameter demonstrates the difference between the linear and non-linear model of a CNT conveying fluid based on the non-linearity of CNT.

3.2. Exact solutions by Jacobian elliptical function method

Let us consider the following non-linear differential equation

$$\ddot{q}(t) + \frac{1+(1+e^2)(K_e+K_p-T-U^2)}{1+e^2}\omega_0^2 q(t) + \frac{\omega_0^2}{4r^2}q^3(t) = 0. \tag{36}$$

The initial conditions are

$$q(0) = a_0, \quad \dot{q}(0) = 0. \tag{37}$$

The exact solution to (36) is expressed as follows

$$q(t) = c_1\,\mathrm{cn}(\omega t + c_2, m), \tag{38}$$

where $\mathrm{cn}(\omega t, m)$ is the Jacobi elliptic cosine function and m is the elliptic modulus. The elliptic modulus and parameter ω are expressed as follows

$$\omega = \sqrt{\frac{1+(1+e^2((K_e+K_p-T-U^2)}{1+e^2}\omega_0^2 + \varepsilon a_0^2}, \tag{39}$$

$$m = \sqrt{\frac{a_0^2\omega_0^2}{8\omega^2 r^2}}. \tag{40}$$

The values of c_1 and c_2 are determined from the initial conditions $q(0) = a_0$ and $\dot{q}(0) = 0$. To find c_1 and c_2, we must solve the system obtained from the initial conditions, i.e.,

$$c_1\,\mathrm{cn}(c_2, m) = a_0, \quad -\omega\,\mathrm{sn}(c_2, m)\,\mathrm{dn}(c_2, m) = \dot{q}(0). \tag{41}$$

From the above equations we get $c_1 = a_0$ and $c_2 = 0$. So the final solution is expressed as

$$q(t) = a_0\,\mathrm{cn}(\omega t, m), \tag{42}$$

where the non-linear frequency of the vibration is given as

$$\omega_{NL} = \frac{\pi\omega}{2\,K(m)}. \tag{43}$$

4. Results and discussion

4.1. Validation

The impacts of different parameters on the non-linear flow-induced frequency of the SWCNT submerged in an elastic medium are evaluated using material and geometrical characteristics from [8]. The CNT is assumed to have Young's modulus of 1 TPa and an effective wall thickness of 10 nm. The inner diameter, the mass density, and the aspect ratio of the SWCNT are 80 nm, 2300 kg/m^3, and 20, respectively. The Winkler and Pasternak constant and the axial tension F are set to be zero ($k_w = k_p = F = 0$) and the fluid inside the nanotube is assumed to be that of water with the mass density 1000 kg/m^3.

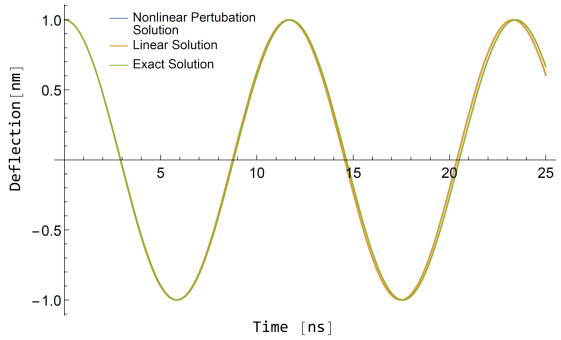

Fig. 2. Comparison of dynamic deflection between the linear, HPM, and exact solution at high flow velocity $U = 0.9$.

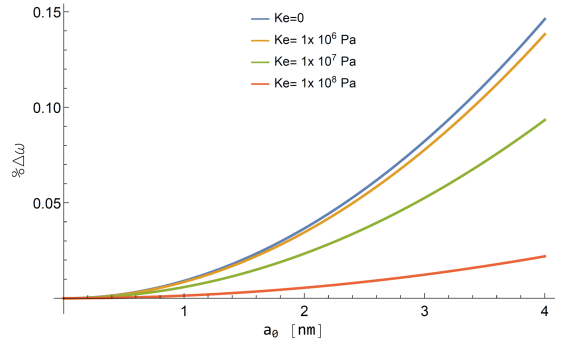

Fig. 3. The non-linear frequency variation $\Delta\omega$ [%] against the maximum non-linear amplitude a_0 with various Winkler constants k_e.

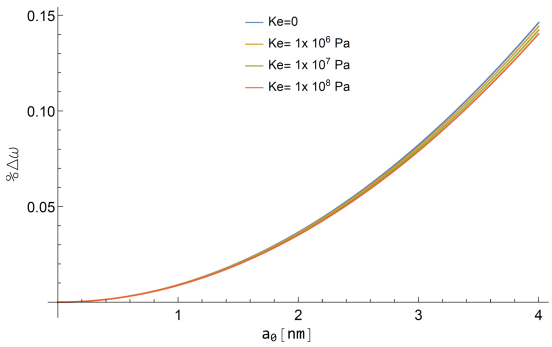

Fig. 4. The non-linear frequency variation $\Delta\omega$ [%] against the maximum non-linear amplitude a_0 with various Pasternak constants k_p.

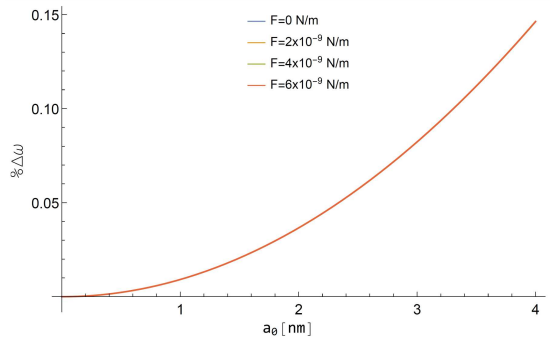

Fig. 5. The non-linear frequency variation $\Delta\omega$ [%] against the maximum non-linear amplitude a_0 with various F.

The dynamic transverse deflection of the SWCNT midpoint is presented in Fig. 2 to test the model's correctness. The results are compared with the linear solution and exact solutions in terms of the Jacobi elliptic functions based on flow velocity ($U = 0.9$). The excellent fit between HPM and exact solutions supports the homotopy perturbation technique's validity. Furthermore, the linear solution predicts a critical flow velocity of 1192.73 m/s, whereas the perturbation technique and exact solutions suggest 1192.84 m/s and 1192.88 m/s, respectively.

4.2. Nonlinear frequency-amplitude relation

The variations between linear and non-linear frequencies were plotted against non-linear amplitude (a_0) concerning the change in the Winkler, Pasternak parameters (k_e, k_p) and axial force F.

Individual plots are demonstrated for each parameter. The effects of the Winkler, Pasternak parameters, and axial forces are presented in the following Figs. 3, 4 and Fig. 5. Figure 3 shows that the increase in the Winkler constant substantially reduces the non-linear frequency. Figure 3 reveals also that at high amplitude, the non-linearity of the model increases linearly when there is no surrounding medium (i.e., $k_e = 0$). For a stiff elastic medium, with an increase in the Winkler constant (i.e. $k_e > 107$ Pa), the non-linear frequency variation decreases. When a nanotube vibrates in a stiff medium, its non-linear frequency tends to become linear. In Fig. 4 the Pasternak constant k_p has very little effect on the non-linear vibration frequency. Figure 5 shows that the effect due to the axial force is very small when compared with the Winkler and Pasternak parameters.

4.3. Nonlinear frequency-flow velocity relation

The variation between the linear and non-linear frequencies is plotted against the dimensionless fluid flow velocity (U) for the Winkler, Pasternak parameters (k_e, k_p) and axial force F, as shown in Figs. 6 and 7.

Individual plots are demonstrated for each parameter. The effects of the Winkler, Pasternak parameters, and the axial forces are presented in Figs. 8, 9 and Fig. 10, respectively. It is observed that at high flow velocity, the non-linear frequency variation is high when there is no surrounding medium or $k_e = 0$. For a stiff elastic medium (i.e. $k_e > 107$ Pa), the variation between the linear and non-linear frequencies remains unchanged. For $U < 0.5$, the percentage of variation remains constant for all values of the Winkler and Pasternak constants. When the constant values decrease,

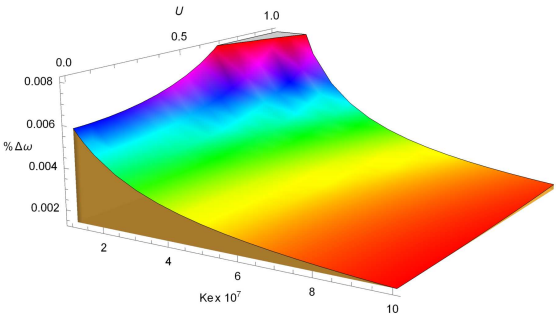

Fig. 6. Three-dimensional plot showing the non-linear frequency variation $\Delta\omega$ [%] against the maximum non-linear amplitude a_0 with various Winkler constants k_e.

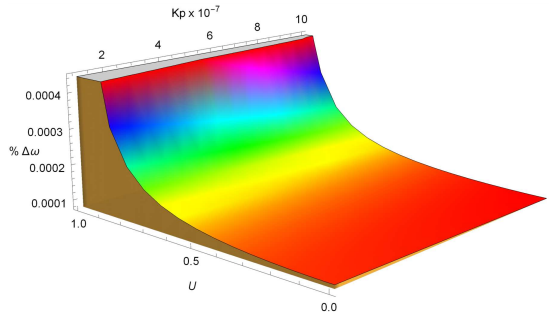

Fig. 7. Three-dimensional plot showing the non-linear frequency variation $\Delta\omega$ [%] against the maximum non-linear amplitude a_0 with various Pasternak constants k_p.

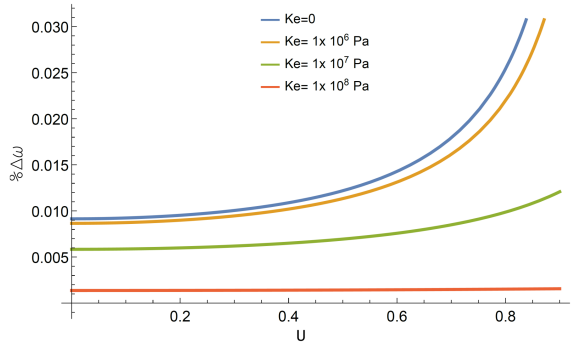

Fig. 8. The non-linear frequency variation $\Delta\omega$ [%] against the maximum non-linear amplitude a_0 with various Winkler constants k_e.

the percentage variation of frequencies increases with the flow velocity U. The value of $\Delta\omega$ [%] declines and remains constant with any increase in flow velocity at low fluid velocities ($U < 0.5$) and as shear stiffness of the elastic medium rises. This demonstrates that the SWCNTs non-linear vibration behaviour is unaffected by the fluid flow and may be ignored in a media with high shear strength. The effects of axial forces show no significant effects in frequency variation.

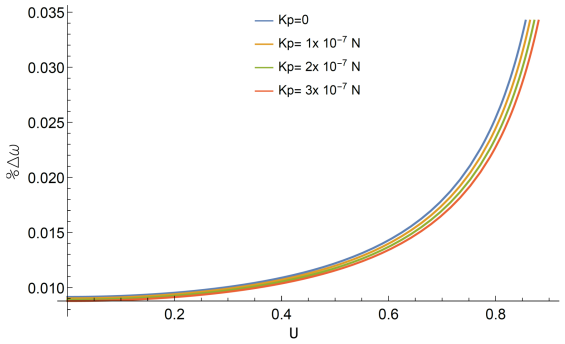

Fig. 9. The non-linear frequency variation $\Delta\omega$ [%] against the maximum non-linear amplitude a_0 with various Pasternak constants k_p.

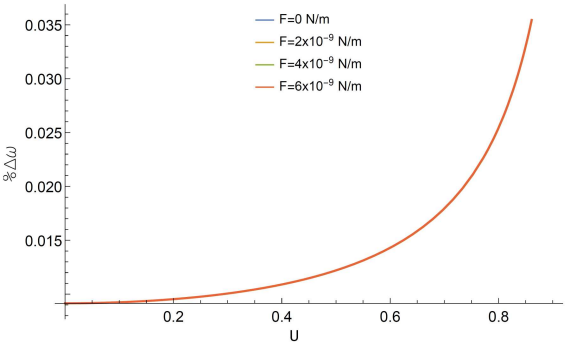

Fig. 10. The non-linear frequency variation $\Delta\omega$ [%] against the maximum non-linear amplitude a_0 with various axial force F.

5. Conclusion

Using continuum theory, a non-linear vibration model of a fluid conveying SWCNT embedded in the Winkler–Pasternak foundation is developed, including the nonlocal elasticity theory. The non-linear equation of motion is solved using the homotopy perturbation method, and the analytical solution is obtained. The Jacobi elliptic functions are used to derive exact answers. Exact solutions in terms of the Jacobi elliptic functions are used to verify the correctness of the results. The results show that:

- At low flow velocities and vibration amplitudes, the variation between the non-linear and linear frequencies is insignificant.
- When the amplitude and flow velocity are both high, the non-linear flow-induced frequency deviates significantly from the linear frequency.
- When CNTs are embedded in media with high Pasternak parameters, the model's non-linearity has no meaningful influence on the frequency.

- At high flow velocity and for large vibration amplitudes, the axial tension limits the nonlinear effect and the flow-induced vibration of the nanotube.

An analytical presentation allows for a better understanding of the system's features and allows for more generalisations to be made. Another possible application of analytical solutions is the provision of accurate reference data for the assessment of numerical methods. The reliable analytical results presented here are deemed beneficial.

References

[1] J.-H. He, *Comput. Meth. Appl. Mech. Eng.* **178**, 257 (1999).

[2] J.-H. He, *Int. J. Non-Lin. Mech.* **34**, 699 (1999).

[3] J.-H. He, *Appl. Math. Computat.* **135**, 73 (2003).

[4] J.-H. He, *Phys. Lett. A* **350**, 87 (2006).

[5] P. Soltani, A. Farshidianfar, *Appl. Math. Modell.* **36**, 3712 (2012).

[6] T. Natsuki, Q.-Q. Ni, M. Endo, *Appl. Phys. A* **90**, 441 (2008).

[7] M. Rasekh, S. Khadem, *J. Phys. D* **42**, 135112 (2009).

[8] J. Yoon, C. Ru, A. Mioduchowski, *Composit. Sci. Technol.* **65**, 1326 (2005).

[9] K. Kiani, *Appl. Math. Modell.* **37**, 1836 (2013).

[10] R. Ansari, A. Norouzzadeh, R. Gholami, M.F. Shojaei, M. Hosseinzadeh, *Physica E* **61**, 148 (2014).

[11] M. Hosseini, M. Sadeghi-Goughari, *Appl. Math. Modell.* **40**, 2560 (2016).

[12] Y.-Z. Wang, Y.-S. Wang, L.-L. Ke, *Physica E* **83**, 195 (2016).

[13] H. Dai, L. Wang, A. Abdelke, Q. Ni, *Int. J. Eng. Sci.* **87**, 13 (2015).

[14] Y.Q. Wang, Y.H. Wan, J.W. Zu, *Thin-Walled Struct.* **135**, 537 (2019).

[15] T.P. Nguyen, T. Nguyen-Thoi, D.K. Tran, D.T. Ho, H.N. Vu, *J. Vibrat. Control* **27**, 1020 (2021).

[16] Y. Amini, M. Heshmati, F. Daneshmand, *Marine Struct.* **79**, 103058 (2021).